ISSN 0001-4338, Izvestiya, Atmospheric and Oceanic Physics, 2014, Vol. 50, No. 8, pp. 776–781. © Pleiades Publishing, Ltd., 2014.
Original Russian Text © A.I. Khlystov, 2014, published in Geofizicheskie Protsessy i Biosfera, 2014, Vol. 13, No. 1, pp. 66–73.

Distribution of Strong and Super Flares by Phases of Solar Activity Cycles

A. I. Khlystov
Sternberg Astronomical Institute, Moscow State University, Moscow, 119992 Russia
e-mail: khlai@rambler.ru

Abstract—The phase distribution of all strong X-ray flares from 1976 to 2013 and the flares in the current 24th cycle have been investigated. It is concluded that, until around 2019, mid-level M-class flares and strong (up to X8 class) flares can be expected. Stronger flares may also occur. Superflares like the Carrington event are unlikely.

Keywords: solar flares, cycle, forecast
DOI: 10.1134/S0001433814080052

INTRODUCTION

Solar radiation measurements conducted with the help of high-precision orbital instrumentation showed that its variation over approximately the past 30 years did not exceed 0.1% according to data available at http://www.pmodwrc.ch (the website of the World Radiation Centre in Switzerland). This is tens of times less than values that could pose a danger to life on Earth (overheating to the boiling point of water during the growth of a radiation flux or a temperature decrease to the level of constant winter under heat deficit). However, the Sun is a highly variable star in the gamma, X-ray, ultraviolet, and radio ranges, where the effective temperature of radiation is sometimes tens and hundreds of times higher than the "optical" effective temperature. The variability is associated with active processes in the solar atmosphere. Among diverse manifestations of solar activity, a special place is occupied by flares as the most powerful nonstationary processes of energy release in the solar atmosphere, affecting all layers of it. Most flares are observed over interfaces of polarity of the large-scale magnetic field of the Sun. Currently, it is believed that these magnetic fields are generated by the dynamo mechanism in a stably stratified narrow transient region between the convection zone with a relatively weak differential rotation and almost rigidly rotating radiative zone below. The model known as the dynamo interface (Spiegel and Zahn, 1992; Parker, 1993; Bushby and Mason, 2004; Thomson, 2004) assumes that the extended poloidal field can generate a toroidal field, which becomes unstable in the course of time due to magnetic buoyancy and rises into the convection zone, acting as a filter and allowing only the strongest field to keep rising to the surface. The areas of magnetic tube rise in the photosphere involve emerging solar spots. Having risen, the magnetic loops fall into the chromosphere and corona and can even enter into interplanetary space.

The motion of magnetized plasma in granules and supergranular cells changes the configuration of magnetic loops: they accumulate a significant amount of magnetic energy, which can be released as a flare through the mechanism of reconnection.

The reconnection of magnetic field lines is the process of converting the magnetic-field energy into other forms of energy due to a change in the topology of the magnetic field. In order for the reconnection process be initiated, an emerging neutral (or zero) point of the so-called X-type, at which the magnetic field vanishes, is necessary. The neutral points (or lines) most often appear from the interaction of magnetic fluxes of opposite polarity. This situation can occur both during a simultaneous rising of opposite-polarity tubes of the magnetic field from below the photosphere and when a new rising magnetic flux is introduced into an existing (old) magnetic field of the active region. Since the magnetic pressure at the X-point (or line) vanishes, the plasma is compressed by an external magnetic field and cooled due to radiation. When critical values of density and temperature are reached, the condition of "freezing-in" of the magnetic field in the plasma is violated and the magnetic-field lines start breaking and joining otherwise in the presence of an electric field. As a result, the energy accumulated in the magnetic field is converted into heat and kinetic energy (Somov, 1993, 2013).

The energy of strong flares can reach 10^{32} erg, which is equivalent to billions of megatons in TNT, and the plasma temperature in the area where the flare was initiated reaches tens or hundreds of millions of degrees (the temperature of thermonuclear fusion) for a short time period. A portion of this enormous energy is spent on radiation in the X-ray and ultraviolet

Strong X-ray solar flares from 1976 to 2006 (according to the catalog available at [http://www.spaceweather.com/solarflares/topflares.html])

Date	Class	Date	Class	Date	Class
04.11.2003	X28+	15.12.1982	X12.9	25.01.1991	X10.0
02.04.2001	X20.0	06.06.1982	X12.0	09.06.1991	X10.0
16.08.1989	X20.0	01.06.1991	X12.0	09.07.1982	X9.8
28.10.2003	X17.2	04.06.1991	X12.0	29.09.1989	X9.8
07.09.2005	X17	06.06.1991	X12.0	22.03.1991	X9.4
06.03.1989	X15.0	11.06.1991	X12.0	06.11.1997	X9.4
11.07.1978	X15.0	15.06.1991	X12.0	24.05.1990	X9.3
15.04.2001	X14.4	17.12.1982	X10.1	05.12.2006	X9.0
24.04.1984	X13.0	20.05.1984	X10.1	06.11.1980	X9.0
19.10.1989	X13.0	29.10.2003	X10	02.11.1992	X9.0

ranges, another portion is spent on the acceleration of protons and electrons (solar cosmic rays and proton events), and yet another portion is converted into the kinetic energy of strong gas flows, resulting in the formation of coronal mass ejections. Each of these components can directly or indirectly have a global impact on the Earth's biosphere, technosphere, and geosphere. As was noted in the 2008 report by the National Academy of Sciences of the United States (http://science1.nasa.gov/science-news/science-at-nasa/2009/21jan_severespaceweather/), "During the following century and a half, with the growth of the electric power industry, the development of telephone and radio communications, and a growing dependence on space-based communications and navigation systems, the vulnerability of modern society and its technological infrastructure to "space weather" has increased dramatically. The adverse effects of extreme space weather on modern technology—power grid outages, high-frequency communication blackouts, interference with Global Positioning System (GPS) navigation signals, spacecraft anomalies—are well known and well documented "Service disruptions of relatively short or conceivably very long duration may spread from a directly affected system to many other systems due to dependencies and interdependencies among, for example, electric power supply, transportation and communications, information technology, and government services." In view of this, the reliable prediction of strong X-ray flares is one important condition for the safe existence of modern civilization.

Since the flares are almost always associated with the magnetic fields on the Sun and spots are a convenient indicator of these fields, it can be expected that the number of flares should correlate with the Wolf numbers (W) characterizing spot activity. To check this assumption, we used the catalog of all strong X-ray flares occurring from 1976 (the year when regular observations of X-ray flares were initiated) to 2006 [http://www.spaceweather.com/solarflares/topflares.html]. The catalog contains 29 strong flares of X9 to X20 class and a single X28+ superflare (see the table).

According to the Solar Influences Data Analysis Center (Brussels, Belgium) [http://sidc.oma.be/], the time interval under consideration covers three (21st, 22nd, and 23rd) solar cycles. Figure 1 shows the time dependence of annual-average Wolf numbers and strong X-ray flares. For clarity, the position of flares on the ordinate axis is bound to the curve of Wolf numbers. Despite the limited amount of available data (3 cycles and 30 flares), we can draw a number of key conclusions:

(1) of all 30 outbreaks in the catalog, only two were observed on the branch of cycle growth; the remaining 28 flares were observed either near the cycle maxima or on the branch of cycle decline;

(2) the number of strong flares per cycle is not correlated with the cycle height: the 21st and 22nd cycles have almost the same height ($W21 = 164.5$ and $W22 = 158.5$), while the number of flares in these cycles differs almost twice (8 flares in the 21st cycle and 14 flares in the 22nd cycle). At the same time, the 21st and 23rd cycles, which significantly differ by height, yielded the same number of flares (8 flares in each cycle);

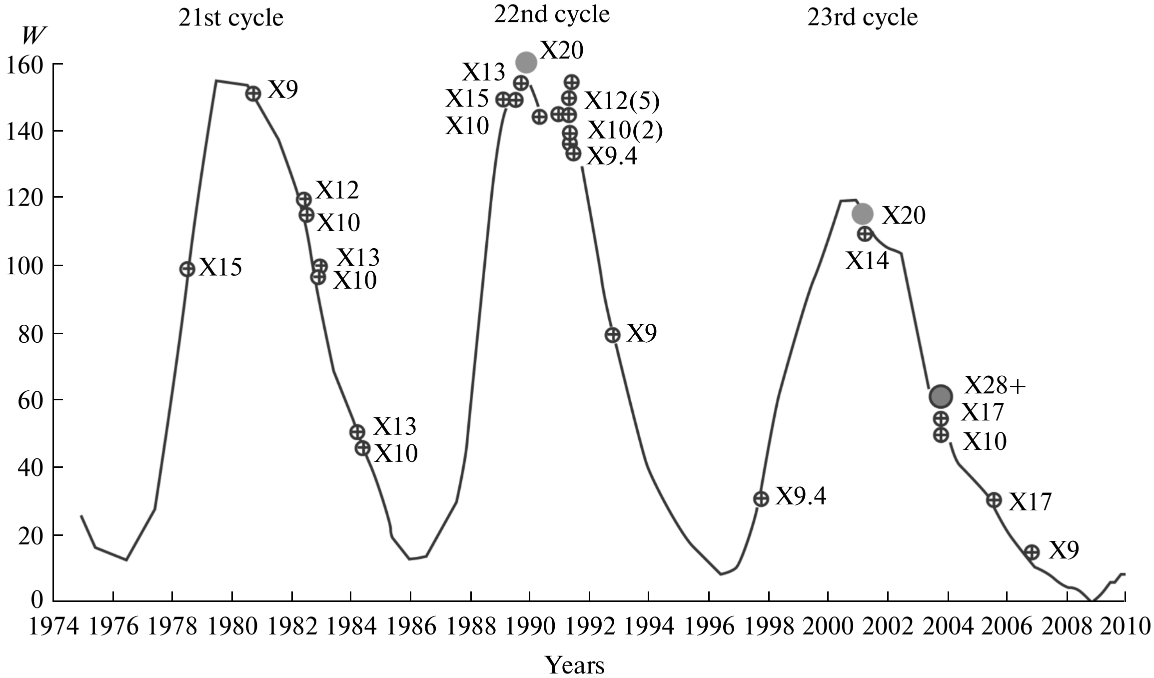

Fig. 1. Time dependence of annual-average Wolf numbers (curve) and distribution of strong X-ray flares from during the 21st, 22nd, and 23rd solar cycles. The power of flares is indicated by their class; the number of flares is given in brackets. The strongest flares are colored.

(3) the lowest (23rd) cycle ($W23 = 120.8$) involved the strongest (for the entire period of observations) flares: two X17 flares, one X20 flare, and an X28+ superflare (most likely, the single superflare of this class over the last 144 years). It should be noted that the higher 21st cycle had no flares stronger than X15 and the class of the strongest flare in the 22nd cycle was X20.

Using the observed course of Wolf numbers from January 2009 to October 2013 [http://www.solen.info/solar/images/cycles23_24.png] (Fig. 2), we have supposed that the maximum of the current (24th) cycle ($W24 = 67$) may have been passed in February 2012. However, in late January 2014 (at the time of final editing of this paper), new data on the course of monthly-average Wolf numbers [http://www.swpc.noaa.gov/ftpdir/weekly/sunspot.gif] allowed us conclude that the 24th cycle will have a second maximum like in the previous cycle. In this case, the position of the new smoothed maximum of the cycle will shift to a later time, which will bring it closer to our earlier prediction (October 2013) (Khlystov and Somov, 2011). It should also be noted that our prediction for the cycle height ($W24 = 63$) almost coincided with observation data (see above).

Thus, the current 24th cycle turned out to be the lowest over the last 110 years and almost twice as low as the 23rd cycle. Can we apply the above-obtained distributions of strong X-ray flares by cycle phases and the conclusion that the flare power is anticorrelated with the cycle height to such a low cycle?

As was stated in (Khlystov and Somov, 2011), a toroidal field is generated from a poloidal field due to differential rotation, i.e., if there is a gradient of the angular velocity of solar rotation by latitude. Since the spots in the early phase of a new cycle normally appear at latitudes of around 30° and then migrate to the solar equator, dropping to ±15° in the cycle maximum and reaching latitudes of ±8° in the cycle end, it can be assumed that the trend of flares to occur near the cycle maximum and on the branch of decline is conditioned by a specific field of velocities in the latitude belt of ±15°. If this assumption is true, it can be concluded that X-ray flares occur either near cycle maxima or on the branch of decline, regardless of the cycle height.

In the current 24th (very low) cycle, the strongest (as of late November 2013) X-ray flare was of X6.9 class and occurred on August 9, 2011, i.e., around six months before the cycle maximum. The second largest flare of class X5.4 occurred near the maximum (on March 7, 2012) and then the flare activity decreased for a long time period until mid-May of 2013. A new surge of activity occurred on May 13–15 of 2013, when a single active region yielded four flares over three days, one of which with X3.2 class become the third largest in the 24th cycle. This series of flares is typical for the phase of the cycle maximum. Until mid-May 2013, there were 51 X-ray flares on the Sun (including medium and weak flares); around 80% of

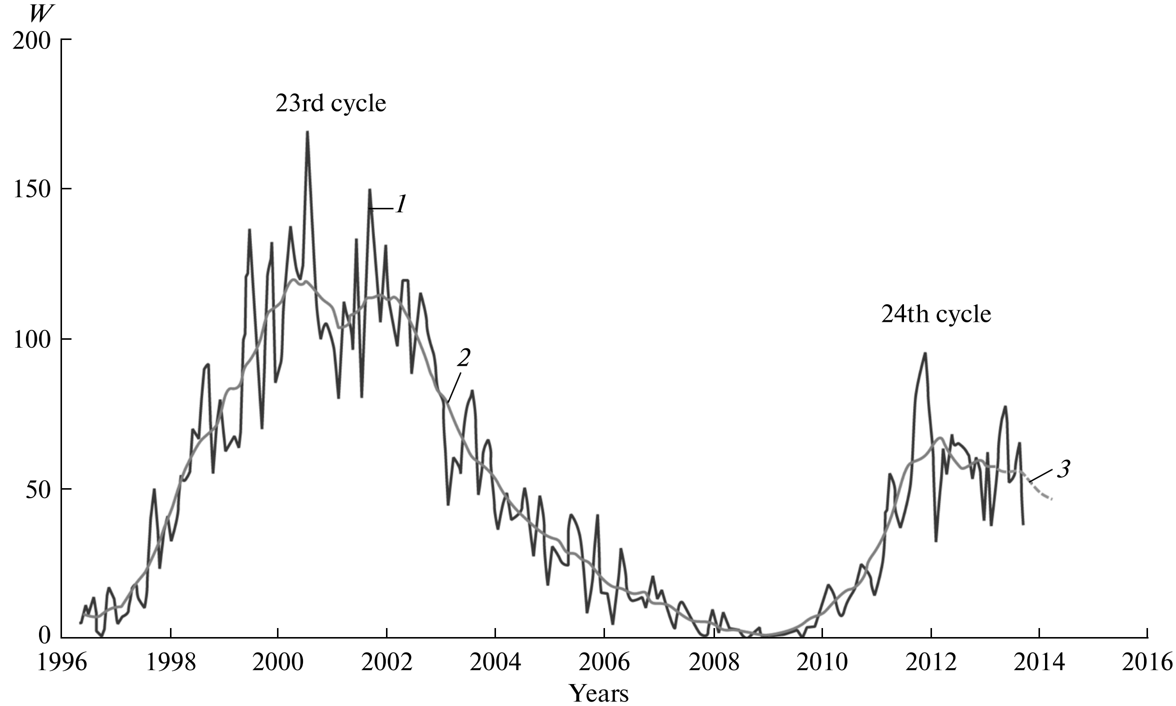

Fig. 2. Time dependence of Wolf numbers in the 23rd and 24th solar cycles: (*1*) monthly average values; (*2*) annual-average values; and (*3*) prediction for 2014.

them were accompanied by coronal mass ejections [http://www.swpc.noaa.gov/alerts/archive.html]. As was noted in (Khlystov and Khlystova, 2012), not all of these ejections are geoeffective (i.e., causing magnetic storms on the Earth), because only part of them are exposed to the Earth's magnetosphere. In our case, approximately half of the coronal mass ejections turned out to be geoeffective (of the 42 recorded events, 20 led to magnetic storms).

Another surge of flare activity started on October 22, 2013 by a series of average-intensity flares of class M, and four strong flares of class X (two X1 and two X2 flares) had occurred on October 25, 28, and 30. In November, this series of flares was supplemented by an X3 flare (November 6) and two X1 flares (November 8 and 10). Thus, the rule of the number distribution of flares by cycle phases, derived by us from data of Fig. 1, is well satisfied for the current 24th cycle as well.

Concerning our conclusion about the possible anticorrelation of flares with the cycle height, it should be noted that this conclusion is not as clear due to the remarkable nonlinearity of the processes involved in the dynamo mechanism (Khlystov and Somov, 2011). It can be expected that it is the 24th cycle (with its anomalously low height) that will bring clarity to this issue. So far, this cycle of activity has had no strong flares (X9 or above); however, according to Fig. 1, it is not improbable that such flares can happen in the nearest future.

Now we consider the possibility of a superflare in the current 24th cycle of activity. The last such flare of class X28+ occurred on November 4, 2003 (see table). The previous superflare, known as the Carrington event (named after Richard Carrington, a British astronomer who observed this activity), occurred on September 1, 1859. By a number of indirect data, the Carrington flare could exceed the power of the November 4, 2003 flare.

Certain hopes for the possibility of predicting the appearance of superflares of the Carrington class can be associated with the so-called barycentric motion of the Sun. Isaac Newton pointed to the fact that mutual gravitational forces affect not only the elliptical motion of planets around the Sun, but the Sun itself must "move in all directions" with respect to the center of mass (barycenter) of the solar system (Cajori, 1934). According to our calculations, such a motion of the Sun is essential for the motion of all planets: the well-known planetary motion along disturbed ellipses around the Sun is supplemented by motion (similar for all planets) due to the barycentric motion of the Sun (Fig. 3). Figure 3 shows that this additional motion occurs with a variable acceleration, which must somehow appear in different planetary environments. Khlystov et al. (2012) compared the observed variations in the angular velocity of the Earth's rotation with the calculated additional accelerated motion of the Earth due to the barycentric motion of the Sun to

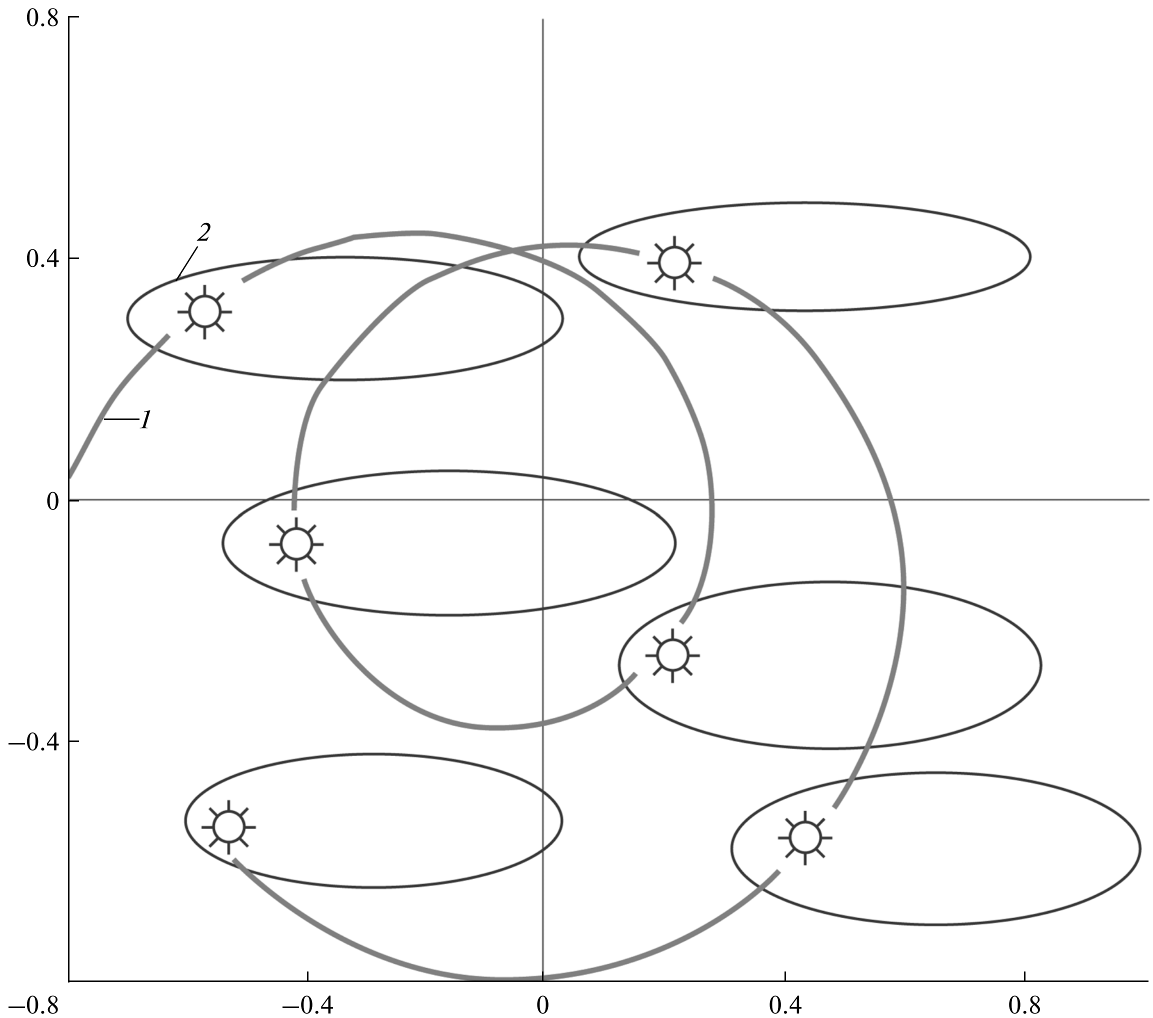

Fig. 3. Combined barycentric motion of the Sun (*1*) and one of the planets of the solar system (*2*) (according to (Khlystov et al., 2012)). The values on the axes are expressed in hundredths of a. u. For clarity, the planet's orbit is highly reduced.

reveal a good correlation between these processes, provided that the barycentric acceleration is mainly contributed by slowly moving distant planets (Saturn, Uranus, and Neptune). Apparently, the interaction between angular velocity of the Earth's rotation and the accelerated barycentric motion has a resonant character leading to the fact that Jupiter, which is closer to the Sun and therefore moving faster, is beyond the resonance region.

We have already mentioned that flares are associated with variations in the angular velocity of the Sun's rotation. It makes sense to assume that, like in the case of the Earth, the accelerated barycentric motion of the Sun can change its angular velocity of rotation, which creates conditions for the emergence of superflares. Since the interval between the two superflares (the 1859 Carrington event and the X28+ giant flare of 2003) is 144 years, according to Table 3 presented in (Khlystov et al., 1992), these superflares could be initiated by the accelerated barycentric motion under the influence of only two large planets (Uranus and Neptune), with a conjunction period of 171.52 years. Figure 4 shows our plot of the change in the Sun's acceleration under the influence of Uranus and Neptune from 1600 to 2200, with an indication of the two strongest superflares (the September 1, 1859 Carrington event and the November 4, 2003 giant flare of class X28+). It can be seen that both superflares occurred near maximum values of the Sun's barycentric acceleration. This allows us to suggest that the X28+ giant flare occurring on November 4, 2003 was another flare of the Carrington type, and the next flare of this kind may occur only in around 144 years (close to 2180). Thus, we believe that the appearance of flares of class $X \geq 28$ or a flare of the Carrington type in the current 24th cycle is unlikely.

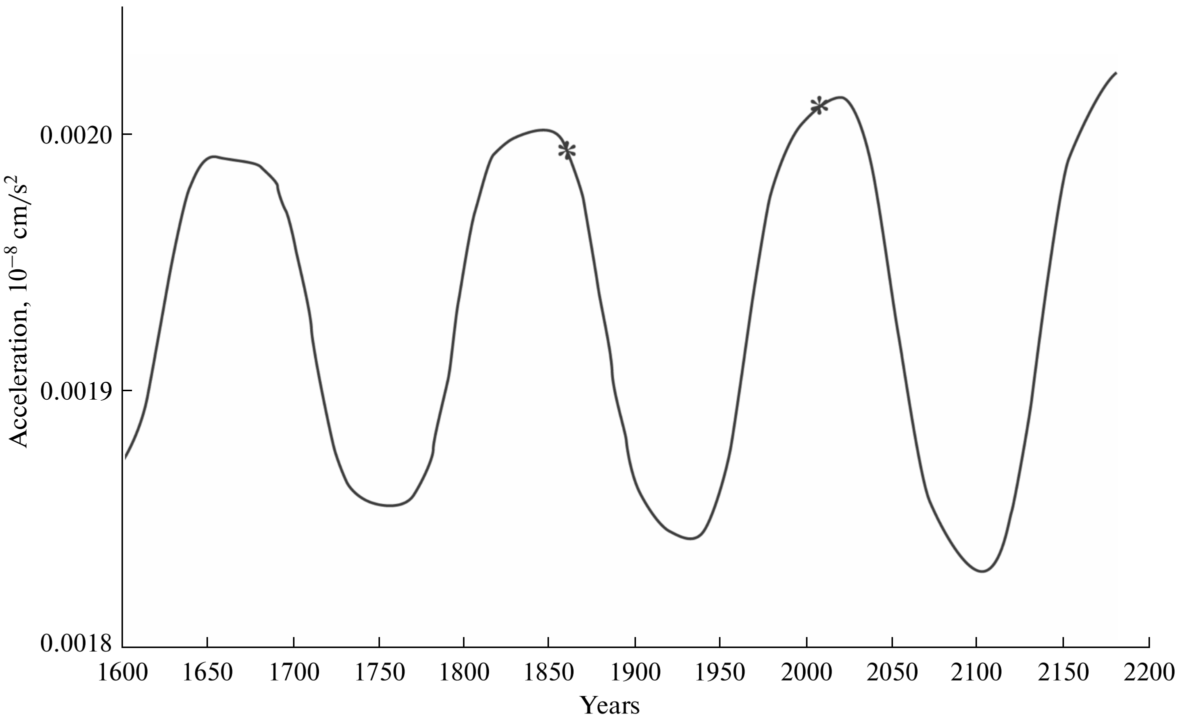

Fig. 4. Change in barycentric acceleration of the Sun under the influence of Uranus and Neptune with an indication of the September 1, 1859 Carrington event and the November 4, 2003 flare as asterisks on the plot.

REFERENCES

Bushby, P. and Mason, J., Understanding the solar dynamo, *Astron. Geophys.*, 2004, vol. 45, no. 4, pp. 4.7–4.13.

Cajori, F., *Newton's Principia*, San Francisco: University of California Press, 1934, Book III, Proposition XIII.

Khlystov, A.I., Dolgachev, V.P., and Domozhilova, L.M., The barycentric motion of the Sun and solar–terrestrial relations, *Biofizika*, 1992, vol. 37, no. 3, pp. 547–553.

Khlystov, A.I., Dolgachev, V.P., and Domozhilova, L.M., The barycentric motion of the Sun and its consequences for the solar system, *Sovremennye global'nye izmeneniya prirodnoi sredy* (Current Global Changes in the Natural Environment), vol. 3: *Faktory global'nykh izmenenii* (Factors of Global Change), Moscow: Nauchnyi mir, 2012, pp. 62–77.

Khlystov, A.I. and Khlystova, V.A., What will do the forthcoming cycle?, *Del'fis*, 2012, no. 1(69), pp. 55–61.

Khlystov, A.I., Klige, R.K., and Sidorenkov, N.S., Type 3 resonance in the solar system, *Sovremennye global'nye izmeneniya prirodnoi sredy* (Current Global Changes in the Natural Environment), vol. 3: *Faktory global'nykh izmenenii* (Factors of Global Change), Moscow: Nauchnyi mir, 2012, pp. 147–160.

Khlystov, A.I. and Somov, B.V., Predicting the main parameters of solar cycle 24 by the number of spotless days in the previous minimum, *Izv., Atmos. Ocean. Phys.*, 2012, vol. 48, no. 7, pp. 717–723.

Parker, E.N., A solar dynamo surface wave at the interface between convection and nonuniform rotation, *Astrophys. J.*, 1993, vol. 408, no. 2, pp. 707–719.

Somov, B.V., *Kosmicheskaya elektrodinamika i fizika Solntsa* (Cosmic Electrodynamics and Solar Physics), Moscow: Izd-vo MGU, 1993.

Somov, B.V., *Plasma Astrophysics*, vol. 2: *Reconnection and Flares*, New York: Springer, 2013.

Spiegel, E.A. and Zahn, J.-P., The solar tachocline, *Astron. Astrophys.*, 1992, vol. 265, pp. 106–114.

Thompson, M.J., Solar interior: Helioseismology and the Sun's interior, *Astron. Geophys.*, 2004, vol. 45, no. 4, pp. 4.21–4.25.

Translated by V. Arutyunyan